Induction of cytotoxicity, apoptosis and cell cycle arrest by 1-t-butyl carbamoyl, 7-methyl-indole-3-ethyl isothiocyanate (NB7M) in nervous system cancer cells

Laurent Brard[†,1]
Rakesh K Singh[†,1]
Kyu Kwang Kim[1]
Thilo S Lange[1]
Giselle L Saulier Sholler[2]

[1]Molecular Therapeutics Laboratory, Program in Women's Oncology, Department of Obstetrics and Gynecology, Women and Infants' Hospital, Brown University, Providence, RI, USA; [2]Department of Pediatrics, University of Vermont College of Medicine, Burlington, VT, USA; [†]These authors contributed equally to the manuscript

Abstract: Our group has recently developed 1-[t]butyl carbamoyl, 7-methyl-indole-3-ethyl isothiocyanate (NB7M), a novel indole ethyl isothiocyanate analog. We now describe its selective cytotoxicity in both central nervous system (CNS) and neuroblastoma (NB) cancer cells. In an effort to understand its mechanism of action we examined the effects of NB7M on apoptosis, cell cycle arrest, and pro-survival/mitogen-activated protein kinase (MAPK) signaling in neuroblastoma cells. NB7M proved highly cytotoxic to NB cell lines (SMS-KCNR, SK-N-SH, SH-SY5Y, IMR-32) with IC_{50} values ranging from 1.0–2.0 μM, whereas lung fibroblasts were less affected ($IC_{50} \geq 10$ μM). In the NCI 60 cell screen 1-dose assay, NB7M (10 μM) reduced the growth (–89 to –27 % growth) of CNS cancer cell lines SF-268, SF-295, SNB-75 (glioblastoma), SF-539 (gliosarcoma), and U251 (astroglioma) while SNB-19 glioblastoma cells were relatively resistant (19% growth). Hoechst staining of SMS-KCNR cells treated with NB7M (3 μM) for 24 hrs exhibited significant chromatin condensation and DNA fragmentation, whereas Annexin-v/7AAD staining revealed that the majority of cells accumulated in the early-apoptotic and late-apoptotic/necrotic stages. NB7M treatment of SMS-KCNR and SH-SY5Y cells also led to the cleavage of procaspases-3, and PARP-1 while causing activation of pro-apoptotic MAPKs and down-regulation of pro-survival factors AKT and PI-3K. Furthermore, NB7M treatment caused S-phase arrest in SMSKCNR and G1-phase arrest in SH-SY5Y cells. NB7M is active against CNS cancers and NB.

Keywords: cytotoxicity, apoptosis, cell cycle analysis, MAPK

Introduction

Cancers of the brain and spinal cord represent the second most common types of cancer affecting children, accounting for 20% of all childhood cancers. About 20% of all brain tumors occur in children younger than 15, usually peaking between ages five and 10. Similarly, neuroblastoma (NB), predominantly a tumor of the peripheral nervous system (PNS), occurs in early childhood and is the most common extracranial solid tumor. Two-thirds of these tumors occur in children younger than age 5. NB accounts for 7%–10% of all childhood cancers; in the majority of patients older than age 1 the disease is fatal (Brodeur et al 2001). Treatment methods currently available include surgery, radiation, chemotherapy, and autologous stem-cell transplantation (Matthay et al 1999; Perez et al 2000). However, despite intensive multimodality treatment, more than 50% of children with high-risk NB relapse, due to drug-resistant residual disease (Perez et al 2000; Goldsby and Matthay 2004). Elimination of refractory microscopic disease remains one of the most significant challenges in the treatment of the high-risk nervous system cancers and innovative treatments are still needed.

Correspondence: Laurent Brard
Assistant Professor of Obstetrics and Gynecology, The Warren Alpert Medical School of Brown University, Director, Molecular Therapeutics Laboratory, Division of Gynecologic Oncology, Department of Obstetrics and Gynecology, Women and Infants Hospital of RI, 101 Dudley Street, Providence, RI 02905, USA
Tel +1 401 453 7520
Fax +1 401 453 7529
Email lbrard@wihri.org; laurent_brard_md@brown.edu

Isothiocyanates (ITCs) are currently being investigated as anti-tumor agents (Kalkunte et al 2006; Satyan et al 2006), and in animal models ITCs have been shown to inhibit chemically induced tumor genesis in the lung, stomach, colon, liver, esophagus, bladder, and mammary glands (Conaway et al 2002). Several mechanisms of action have been proposed, including (i) induction of apoptosis and G2/M cell cycle block (Jackson et al 2007), (ii) inhibition of phase-I and -II carcinogen-activating enzyme (Dick and Kensler 2002), (iii) increase in nuclear content of NF-κB (Jakubikova et al 2006), (iv) inhibition of histone deacetylase (Jakubikova et al 2005) and (vi) up-regulation of thioredoxin reductase-1 (Johnson et al 2004). Various other effects such as disruption of microtubulin polymerization (Jackson and Singletary 2004) and disruption of mitochondrial membrane potential have been reported (Yuesheng et al 2003). Moreover, naturally occurring ITCs (Figure 1) inhibit activation and/or function of factors implicated in the emergence of multi-drug resistance (Tseng et al 2004).

Naturally occurring indole derivatives, such as Indole-3-carbinol, exhibit potent antiproliferative activity, induce apoptosis, and cause cell cycle arrest in many human solid and nonsolid tumors (Garcia et al 2005). Recently, we described the identification of a novel indole scaffold-based isothiocyanate class of potent cytotoxic agent (7Me-IEITC) which showed potent antitumor activities in both high risk neuroblastoma (Singh et al 2007) and platinum-resistant ovarian cancer (Singh et al 2008). Interestingly, further structural optimization by tert-butyloxycarbonyl (tBOC) protection of the indole nitrogen led to the identification of a more potent analog (NB7M; Figure 1) which has recently shown a broad range of antitumor activity in the NCI 60 cell *in vitro* screen 1-dose assay against multiple cancer cell-types, including central nervous system (CNS) cancers. Furthermore, we have recently investigated the *in vitro* cellular apoptotic effects of NB7M in platinum-resistant ovarian (SKOV-3) cancer cells (unpublished).

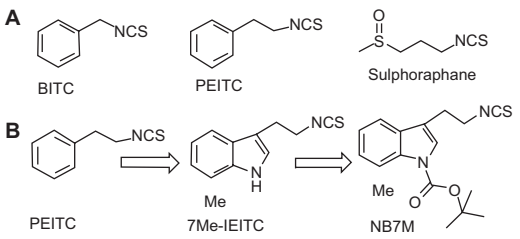

Figure 1 Naturally occurring ITC; design and structure of novel Indole ethyl ITC (IEITC). (**A**) Various naturally occurring ITC: (i) BITC; (ii) PEITC; (iii) Sulforaphane. (**B**) Design of novel Indole ethyl isothiocyantes (IEITC) leading to NB7M.

The primary objective of the present study was to investigate the cytotoxic effects of NB7M against both high risk CNS cancer cell lines and neuroblastoma. This was accomplished by (i) screening NB7M against a panel of CNS cancer and neuroblastoma cell lines, (ii) defining its antiproliferative and apoptotic effects in conjunction with key signaling changes in SMS-KCNR and SH-SY5Y NB cells, and (iv) by studying its effects on cell cycle progression.

Material and methods

Cell lines (human)

The human neuroblastoma cell lines SK-N-SH, IMR-32, SH-SY5Y (ATCC, Manassas, VA), SMS-KCNR (gift from John Maris, Children's Hospital of Philadelphia, Philadelphia, PA), and MRC-5 human lung fibroblasts, (ATCC, Manassas, VA) were maintained in RPMI 1640 media supplemented with 10% (v/v) fetal bovine serum, 100 units/ml penicillin and 100 μg/ml streptomycin at 37 ºC in a 5% CO_2, humidified incubator. SH-SY5Y cells were grown in complete DMEM media (10% FBS+100 units/mL penicillin and 100 μg/mL streptomycin, supplemented with 1% MEM NEAA, catalog #11140, Invitrogen). Cells were then grown in T75 cell culture flasks (Corning, New York, NY) to ~80% confluency in complete medium (Gibco, Rockville, MD). For all assays, cells were allowed to attach overnight and treated in complete RPMI medium. Details regarding the maintenance and handling of CNS cancer cells lines used in NCI 60 cell screen 1-dose assay are available at http://dtp.nci.nih.gov.

Cell viability assay

Viability of cells was determined by the 96® Aqueous-One-Solution Assay (Promega, Madison, WI). This colorimetric assay is based on the ability of mitochondria to reduce a substrate (MTS) into a soluble formazan product with an absorbance at 490 nm (ELISA plate reader; Thermo Labsystems, Waltham, MA) directly proportional to the number of living cells (Malich et al 1997). Cells (5×10^3) were plated in 96-well flat bottom plates (Corning, Inc., Corning, NY) and treated with NB7M. Experiments were performed in triplicates; data are expressed as the mean of the triplicate determinations (X ± SD) of a representative experiment in % of absorbance of samples with untreated cells (100%).

Measurement of mitochondrial transmembrane potential

Variations in mitochondrial transmembrane potential (ΔYm) during the induction of apoptosis were examined using 3,3-dihexyloxacarbocyanine iodide (DiOC63) (Invitrogen,

Oregon, USA). Cells (1×10^6) were seeded in a 100 mm Petri dish and treated with media alone or with of NB7M (1.5 μM) for 4 or 12 hrs. Following treatment, cells were washed with phosphate buffer solution (PBS), re-suspended in fresh medium (5×10^5 cells/mL) and incubated with 15 nM DiOC63 for 30 min at 37 °C. The cells were then washed twice with DPBS, re-suspended in equal volumes of DPBS and DiOC63, and measured by flow cytometry (excitation = 488 nm, emission = 520 nm). Data was acquired on a BD FACSort flow cytometer using CellQuest software (BD Immunocytometry-Systems, San Jose, CA) and analyzed (ModFit LT software, Verity Software House, Inc., Topsham, ME). Ten thousand cells were analyzed for each sample.

Morphological studies

Cells were seeded (1×10^4/chamber) in a Lab-Tek Chamber-Slide System (Nalge Nunc., Naperville, IL) and treated for 24 hrs with 2 μM of NB7M. Following two washes with PBS, cells were fixed in PBS, 2% PFA, 0.2% Triton X for 20 min at room temperature and stained for 10 min with 200 ng/mL Hoescht in PBS before mounting. Representative images were taken with an inverted microscope (Nikon Eclipse TE2000-E, CCD camera) and 20X objective.

Apoptosis (AnnexinV assay) by FACS analysis

SMS-KCNR cells (1×10^6) were seeded in a 100 mm^2 Petri dish and treated with NB7M (0, 1.5, and 3 μM) for 24 hrs. Following treatment, cells were washed twice with cold PBS, re-suspended in binding buffer (1X) at a concentration of 1×10^6 cells/mL. 100 μL of the cell suspension (1×10^5) was transferred to a 5 mL culture tube. Five μL of AnnexinV-PE and 5 μL of 7-AAD were added to each tube. Cells were gently vortexed and incubated with for 15 min at room temperature (25 °C) in the dark. Next, 400 μL of binding buffer (1X) was added to each tube and the cell suspension was subsequently analyzed by flow cytometry (excitation = 488 nm, emission = 520 nm). Data was acquired on a BD FACSort flow cytometer using CellQuest software (BD Immunocytometry-Systems, San Jose, CA) and analyzed (ModFit LT software, Verity Software House, Inc., Topsham, ME). Ten thousand cells were analyzed for each sample.

Western blot analysis

Cells were seeded in 100 mm^2 tissue culture dishes (5×10^5 cells/dish), cultured to ~80% confluency, and treated as indicated. The cells were then rinsed in PBS, pH 7.4, scraped, spun down in a microcentrifuge (10,000 g, 5 min) and cell pellets re-suspended in lysis buffer (1%NP-40, 20 mM Tris pH 8.0, 137 mM NaCl, 10% glycerol, 2 mM EDTA, 1 mM activated sodium orthovanadate, 10 μg/mL Aprotinin, 10 μg/mL Leupeptin, Inhibitor Cocktail P-2714; Sigma-Aldrich, St. Louis, MO). Lysates were rocked at 4 °C for 5 min, sonicated (10 pulses 5 sec), centrifuged at 14,000 g for 10 min, and the protein concentration of the supernatant quantified (BioRad protein estimation kit, Hercules, CA). The samples were boiled in the presence of 5X SDS-PAGE sample buffer to achieve a final concentration of 1X and 50 μg total protein/lane were separated on 12% SDS-polyacrylamide gels and blotted onto PVDF membranes. The blots were blocked with 5% nonfat dry milk in PBST for 1 hr at room temperature and incubated overnight at 4 °C with antibodies specific for pro-caspase-3, cleaved caspase-3, phosphorylated and total p38, JNK1/2, ERK1/2, PI3-K, Akt, and STAT-3 (purchased from Cell Signaling Technology, Beverly, MA or Amersham-Pharmacia Biotech, Piscataway, NJ) at a 1:1000 dilution in 5% BSA in PBST on a rotating platform. Actin was probed using mouse anti-actin antibodies (Sigma Chemical Company, St. Louis, MO) and used as internal loading control. The protein bands were photographed (BioRad, Gel Document System, GDS 8000). After washing in PBST, the blots were incubated with secondary antibodies (peroxidase-conjugated antibodies; Amersham-Pharmacia Biotech, Piscataway, NJ). The bands were visualized by enhanced chemiluminescence and autoradiography (F-Bx810 Film, Pheonix, Hayward, CA). As a size standard, pre-stained Precision plus Protein Kaleidoscope (Biorad, Hercules, CA) marker was used.

Cell cycle analysis (by FACS)

Cell cycle analysis and quantification of apoptosis was carried out by flow cytometry. Cells were seeded in 100 mm^2 tissue culture dishes (7.5×10^5 cells/dish), allowed to attach overnight, and treated for 12 and 24 hrs (500 nM and 1.0 μM). At the end of the incubation period, detached cells were collected in 15 mL polypropylene centrifuge tubes along with the medium; culture dishes were washed once with PBS, adherent cells scraped off and combined in the same tube. After centrifugation (250 g, 5 min) cells were fixed (ice-cold 70% ethanol for 30 min) followed by incubation with 50 μg/mL of propidium iodide and 100 μg/mL of RNase for 30 min at 37 °C in the dark. Data was acquired on a BD FACSort flow cytometer using CellQuest software (BD Immunocytometry Systems, San Jose, CA) and analyzed using ModFit LT software (Verity Software House,

Inc., Topsham, ME). Ten thousand events were analyzed for each sample. Appropriate gating was used to select the single cell population NB cells. The same gate was used on all samples, ensuring that the measurements were made on a standardized cell population.

Data analysis

Mean and standard deviation (SD) were calculated. Mean differences were determined by Student's t-test or determined by one-way ANOVA, using the Newman-Keuls test to account for multiple comparisons in post hoc analyses. Software used for these analyses was GraphPad Prism 3.0 (San Diego, CA).

Results

NB7M is cytotoxic to both CNS cancer and neuroblastoma cell lines

As an initial approach to evaluation of antitumoral activity of NB7M, a cell viability assay (Malich et al 1997) of various neuroblastoma cancer cell lines treated with NB7M was carried out. NB7M dose-dependently reduced the viability of all NB cell lines SMS-KCNR, SH-SY5Y, IMR-32, and SK-N-SH (IC_{50} below 1.0 μM; Figure 2A). NB7M was selectively cytotoxic for NB cells. The viability of primary lung fibroblasts (MRC-5, passage 10), which like NB cell lines possess a high metabolism and growth rate and, thus, were used as controls, were not affected by NB7M treatment (Figure 2A drug concentrations as high as 10 μM).

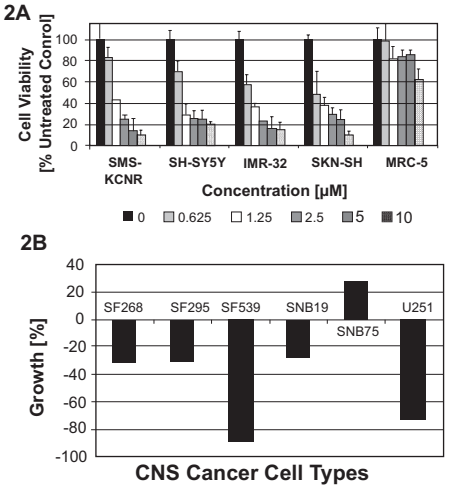

Figure 2 Comparative analysis of the cytotoxic effect of NB7M in a human NB cell lines (SMS-KCNR, SH-SY5Y, IMR-32, SK-N-SH). **Panel A:** NB cells were treated with various concentrations (0.625 μM to 10 μM) of NB7M for 48hrs. Viability was measured using the MTS assay (see Materials and methods). Experiments were performed in triplicates; data are expressed as the mean of the triplicate determinations (X ± SD) of a representative experiment in % cell viability of untreated cells (100%). **Panel B:** CNS cancer cells were treated with NB7M (10 μM) for 48 hrs and the cell growth measured according to the NCI/DTP assay (see http://dtp.nci.nih.gov/docs/cancer/cancer_data.html for details).

Given its activity against NB cells, we were interested in the effects of NB7M against CNS cancer cells. To this end, NB7M was submitted to the NCI Developmental Therapeutics Program (http://dtp.nci.nih.gov) and screened against a panel of 60 cancer cell lines. This panel consists of well characterized CNS cancer cell lines such as SF-268, SF-295, SNB-19, SNB-75 (glioblastomas), SF-539 (gliosarcoma), and U251 (astroglioma). Following an initial 1-dose screen (10 μM, per NCI-DTP protocol), NB7M was selected for 5-dose screening and all cancer cell lines and these results are currently pending. Analysis of the 1-dose assay revealed that SF-268, SF-295, SF-539, SNB-75 and U251 were sensitive (–89% to –27 growth, Figure 2B) to NB7M treatment, whereas, SNB-19 (adherent fibroblastic cells of human glioblastoma) were relatively insensitive (19% growth). NB7M appears to be a potent cytotoxic agent against nervous system cancer cells.

NB7M affects mitochondrial membrane depolarization potential and produces morphological hallmarks of apoptosis in SMS-KCNR cells

We next focused our efforts on the effects of NB7M on NB cells, and specifically SMS-KCNR cells (a known chemotherapy-resistant cell line). To understand the effects of NB7M on cellular functions, we measured the integrity/loss of mitochondrial transmembrane depolarization potential ($\Delta\Psi m$). NB7M treatment of SMS-KCNR cells resulted in a time-dependent increase in the number of cells with $\Delta\Psi m$. After 4 hrs, 20% of the cells, and by 12hrs, 26% of the cells had lost their Ψm (Figure 3A). Even within the population of remaining cells (74%), fluorescent staining with DiOC6(3) showed a broader distribution of intensity compared with nontreated cells, indicating an altered mitochondrial transmembrane depolarization potential (Figure 3A, insert at top of bar diagram).

To visualize nuclear changes and apoptotic body formation that are characteristic of apoptosis, SMS-KCNR cells treated with NB7M (3 μM, 24 hrs) were stained with Hoechst 33258 staining (Kasibhatla et al 2006). This bisbenzimidazole dye is known to penetrate the plasma membrane and stain DNA in cells without permeabilization. In this assay, apoptotic cells have a stronger blue fluorescence compared with nonapoptotic cells. In contrast to control cells, NB7M-treated cells exhibit highly condensed chromatin that

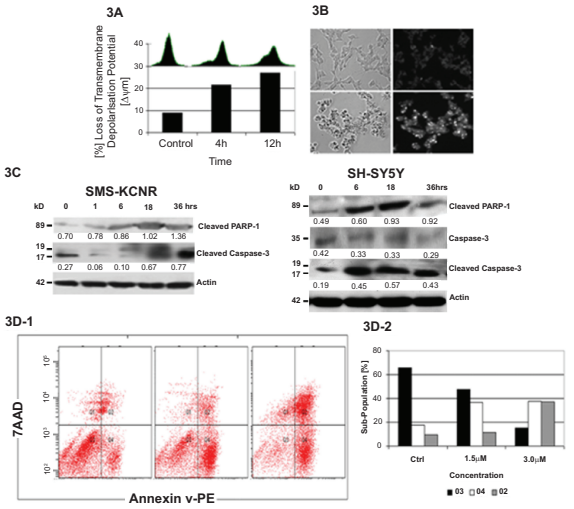

Figure 3 NB7M causes apoptosis in neuroblastoma cells. **Panel A:** Loss of transmembrane depolarization potential in SMS-KCNR cells. Cells were treated with NB7M (1 μM) for 4 and 12 hrs and an increase in the percentage of cells with reduced transmembrane potential is noted. All experiments were performed in duplicate. **Panel B:** SMS-KCNR cells were treated with NB7M (3 μM) for 24 hrs. Treated cells (bottom images) reveal disrupted cell structure and chromatin condensation as compared to untreated cells (top images). All experiments were performed in duplicate. **Panel C:** SMS-KCNR and SH-SY5Y cells treated with NB7M (1.5 μM) exhibit the release of cleaved PARP-1, and activation of cleaved caspase-3 (19 and 17 kD). Actin was used as an internal standard of protein loading. Numerical ratios of band intensities relative to actin are presented. All experiments were performed in duplicate. **Panel D:** SMS-KCNR cells treated with NB7M (0, 1.5 and 3.0 μM, left-to-right, **3D-1**) reveal a concentration-dependent increase in apoptotic cell populations. The same results is shown in graph form (**3D-2**).

was uniformly stained by Hoechst 33342 (Figure 3B). Based on these morphologic findings, NB7M appears to cause apoptosis in SMS-KCNR cells.

Apoptosis is executed by caspases. Initiator caspases (such as caspase-2, –8, –9, and –10) function mainly as upstream apoptotic signals. Once activated, the initiator caspases cleave and activate downstream effector caspases (such as caspase-3, –6, and –7), that are responsible for the cleavage of many intracellular proteins, ultimately leading to the morphological and biochemical changes associated with apoptosis (Salvesen and Abrams 2004). Accordingly, immunoblotting of lysates of SMS-KCNR and SH-SY5Y cells confirmed that NB7M treatment resulted in strong activation/cleavage of caspase-3 (Figure 3C) and PARP-1, another hallmark of apoptosis. Furthermore, within 3, 12, and 24 hrs of the NB7M treatment (1 μM), 24%, 39%, and 42% cells lost the membrane depolarization potential, which is an indicator of the integrity and health of the cells and indicates how rapidly NB7M can induce the apoptotic events. The direct consequence of the induction of apoptosis by NB7M is the reduction of viability in NB cells as demonstrated in (Figure 2A).

To further understand the effects of NB7M on cell death and specifically to distinguish between apoptosis and necrosis, two major cell death pathways, NB7M (1.5 and 3.0 μM) treated cells were stained with Annexin-V and propidium iodide (Van et al 1996). Apoptosis is an active, genetically regulated, disassembly of the cell from within. Disassembly creates changes in the phospholipid content of the cytoplasmic membrane outer leaflet. Phosphatidylserine (PS) is translocated from the inner to the outer surface of the cell for phagocytic cell recognition. The human anticoagulant, annexin-V, is a 35 kD Ca^{2+}-dependent phospholipid protein with a high affinity for PS. Annexin V labeled with fluorescein (FITC) ($\lambda_{abs}/\lambda_{em}$ = 492/514 nm) can identify apoptotic cells with green fluorescence by binding to PS exposed on the outer leaflet. On the other hand, necrosis normally results from a severe cellular insult. Both internal organelle and plasma membrane integrity are lost, resulting in spilling of cytosolic and organellar contents into the surrounding environment. Propidium iodide is a highly positively charged nucleic acid probe that is membrane impermeant and generally excluded from viable apoptotic cells, but stains necrotic cells with red fluorescence ($\lambda_{abs}/\lambda_{em}$ (intercalated with DNA) = 528/617 nm). The combination of annexin-V/PI provides a convenient way to quantify apoptotic (green) and necrotic (red) cells within the same cell population by flow cytometry. NB7M treatment of SMS-KCNR caused a concentration dependent increase in annexin V and PI staining (Figure 3D). Within 24 hrs of NB7M (3 μM) treatment, approximately 40% of SMS-KCNR cells were labeled with annexin-V (early apoptosis), 39% cells were stained with propidium iodide (late apoptosis and necrosis), and only a small cell population remained unlabeled (with either annexin-V or PI) compared with the untreated control cells (Figure 3D).

NB7M downregulates pro-survival signals and upregulatess pro-apoptotic signals in SMS-KCNR and SH-SY5Y cells

To define the cellular response of NB cells to treatment with NB7M, we analyzed the expression and/or activation of cellular markers that are hallmarks of pro-survival (Akt), and pro-apoptotic signaling (JNK, p38 MAPK) in both SMSKCNR and SH-SY5Y cells.

The effect of NB7M on the activation/phosphorylation of JNK, p38 MAPKs and Akt was studied by immunoblotting of PAGE separated lysates of treated cells using antibodies specifically recognizing the inactive, as well as the phosphorylated active forms of these proteins. NB7M caused strong activation of p38 and JNK MAPKs along in both SMS-KCNR and SH-SY5Y cells (Figure 4A).

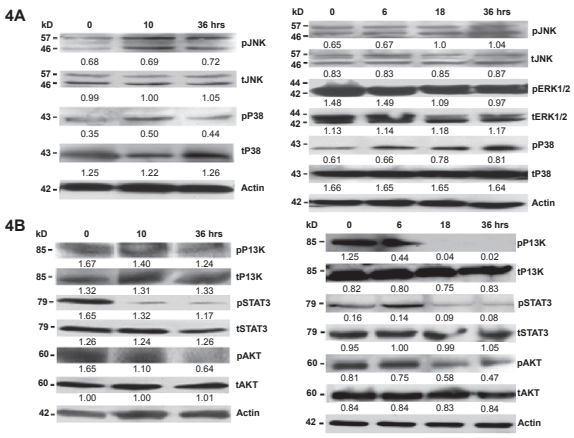

Figure 4 Effect of NB7M on signaling proteins. **Panel A:** expression of apoptotic markers in NB cells after NB7M treatment. SMS-KCNR and SH-SY5Y cells were treated with 1.5 μM of NB7M. Actin was used as an internal standard of protein loading. Numerical ratios of band intensities relative to actin are presented. All experiments were performed in duplicate. **Panel B:** expression of pro-survival markers in NB cells after NB7M treatment: SMS-KCNR and SH-SY5Y NB cells were treated with 1.5 μM of NB7M. Actin was used as an internal standard of protein loading. Numerical ratios of band intensities relative to actin are presented. All experiments were performed in duplicate.

This figure also shows that SMS-KCNR and SH-SY5Y cells possess an elevated basal level of activation/phosphorylation of pro-survival factor Akt in untreated cells that is down-regulated within 36 hrs of NB7M treatment.

Next, we investigated signal transducer and activator of transcription 3 (STAT-3) protein expression in NB (SMS-KCNR and SH-SY5Y) cells treated with NB7M. STAT-3 is activated in diverse human tumors and may play a direct role in malignant transformations. Various inhibitors of STAT-3 protein and STAT-3 pathways have been identified and shown, both *in vitro* and *in vivo*, to possess antitumor activities (Barre et al 2006). We investigated the effect of NB7M treatment on the expression profile of STAT-3 in both SMS-KCNR and SH-SY5Y cells by Western blot analysis (Figure 4B). NB7M treatment significantly reduced the phosphorylation of STAT-3 in resistant phenotypic SMS-KCNR cells. Similarly, the phosphorylation of STAT-3 in SH-SY5Y cells was down-regulated by 18–36 hrs following NB7M treatment. Our results indicate that NB7M is a micromolar antagonist of STAT-3 phosphorylation/signaling.

NB7M arrests the cell cycle progression of SMS-KCNR cells in S phase and G1 arrest in SH-SY5Y cells

NB7M acts as a cytotoxic drug and leads to a protein expression profile characteristic of apoptotic events. Based on our previous work (Singh et al 2007), we hypothesized that NB7M should affect cell cycle progression in SMS-KCNR and SH-SY5Y cells. To test this hypothesis, we analyzed the cell cycle progression of SMS-KCNR and SH-SY5Y cells treated with NB7M. Treatment of SMS-KCNR and SH-SY5Y cells with NB7M (1.0 and 0.5 μM, respectively) leads to a preponderance of cells in the apoptotic sub-G0/G1 (Figure 5) within 12 hrs. The apoptotic sub-G0/G1 population represents cells with significant DNA damage. This observation directly correlates with the reduction of SMS-KCNR and SH-SY5Y cells viability by NB7M at concentrations of 625 nM to 1.25 μM (Figure 2A). With respect to cycling cells, NB7M treatment of SMS-KCNR cells for 12 hrs caused a significant increase of cells in S-phase, whereas SH-SY5Y cells were arrested in the G1-phase with concomitant increase in the sub-G0/G1 population and decrease in the S-phase population (Figure 5). Apparently, in this asynchronous cell culture, NB7M treatment affected cell-cycle checkpoints in G2/M and S-phases causing a reduction of cell-cycle progression along with transition to the apoptotic stage. Even though not the objective of the present report, further studies emphasizing cancer related cell cycle features (Mazumder et al 2004) could focus on the specific checkpoints in G1/S and G2/M phase affected by sub-cytotoxic NB7M treatments. This would require the study cell cycle regulators (cyclin-dependent kinases and cyclins) (Pines 1999) in synchronized neuroblastoma cultures.

Discussion

NB7M is a novel synthetic indole ethyl isothiocyante analog, which was synthesized by incorporating an additional

5A

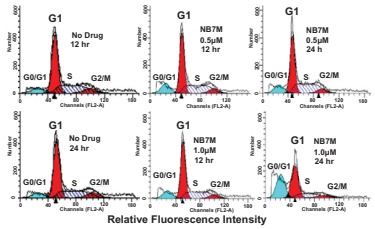

5B

SMS-KCNR cells		G1-Phase [%]	S-Phase [%]	G2/M Phase [%]	Sub-G1 Phase [%]
No Drug	12 hrs	56.0	9.6	34.4	8.8
	24 hrs	52.6	9.3	38.8	6.8
0.5 μM	12 hrs	51.1	14.4	34.4	6.8
	24 hrs	47.8	36.9	15.4	12.9
1.0 μM	12 hrs	53.1	34.4	12.4	13.9
	24 hrs	53.4	24.2	2.2	29.8
SH-SYSY cells		**G1-Phase [%]**	**S-Phase [%]**	**G2/M Phase [%]**	**Sub-G1 Phase [%]**
No Drug	12 hrs	56.8	33.7	9.4	8.8
	24 hrs	56.9	32.8	10.2	8.2
0.5 μM	12 hrs	51.4	41.2	7.2	12.4
	24 hrs	53.2	38.6	8.0	14.4
1.0 μM	12 hrs	57.3	34.2	8.4	13.3
	24 hrs	62.6	27.3	9.9	35.6

Figure 5 NB7M effect on cell cycle progression in NB cells. Cell Cycle analysis by FACS: SMS-KCNR and SH-SY5Y NB cells were treated with NB7M (0, 0.5, and 1.0 μM) for 12 or 24 hrs. Cell cycle analysis of treated and untreated cells was performed. Data are presented as the relative fluorescence intensity of cell sub-populations in the 2-dimensional FACS profile or in percentage of cells in a given sub-population.

tert-butyl carbamate group to protect the *sec*-amino group of 7Me-IEITC (Figure 1). 7Me-IEITC itself is a potent anti-tumor agent that showed potent antineuroblastoma (Singh 2007) and antiovarian cancer activities (Singh et al 2008). The rational for adding a tert-butyl carbamate group was to protect the *sec*-amino group of 7Me-EITC, thereby, possibly resulting in better pharmacokinetic and pharmacodynamic properties (Serova et al 2007).

NB7M has shown promising *in vitro* cytotoxicity in many well characterized human solid tumor cancer cell lines collectively known as 'NCI60 cell lines' which broadly represent tumors of organs such as lung, ovarian, prostate, skin and renal, prostate, breast, colon, central nervous system, and leukemia. Most of these cell lines are representative of tumors warranting the development of novel anticancer agents due to the current lack of efficacious drugs. NB7M exhibited potent *in vitro* activity against many central nervous system cancer cell lines such as SF539 (–89% growth) and U251 (–73% growth). A comparison analysis of cytotoxicity of various drugs in clinical use (data available at NCI-DTP website) indicates that NB7M is more potent than current drugs in clinical use (eg, cisplatin, oxiplatin, seliciclib, CNDAC, 5Fu, and cyclophosphamide) in most of the cell lines but is less potent than doxorubicin, docetaxel, and gemicitabine. Additionally, the cytotoxic potential of NB7M against neuroblastoma cancer cell lines (SMS-KCNR, SK-N-SH, IMR-32, and SH-SY5Y), which are not represented in NCI60 panel, were also investigated. All four cell lines were highly sensitive to NB7M treatment ($IC_{50} < 1.0–1.5\ \mu M$). The cytotoxicity profiles of the other isothiocyanate analogs tested, including 7Me-IEITC and PEITC, appeared to partially differ from that of NB7M suggesting differences in the metabolism, mechanism of action and/or resistance between NB7M and these other isothiocyanate analogs (Singh et al 2007).

Our *in vitro* investigations have shown that even though NB7M and 7Me-IEITC (Singh et al 2007) display overlapping cytotoxic effects in the case of SH-SY5Y and IMR-32, SMS-KCNR cancer cells were more sensitive to NB7M than 7Me-IEITC. Sapacitabine (Serova et al 2007), a N4-protected analog, exhibited similar selective cytotoxicity profiles when compared with structurally related nucleoside analogs. NB7M displayed cytotoxic effects against most of the cancer cell lines tested irrespective of the origin of the tumor and usually at lower concentrations than that required for 7Me-IEITC and PEITC (a naturally occurring anticancer ITC). It is not surprising that NB7M and 7Me-IEITC display overlapping cytotoxic effects, especially if the later is a metabolite of the former. However, differences observed between those two compounds suggest that NB7M may act as a metabolite of 7Me-IEITC but also by its own mechanisms of action. It remains to be demonstrated whether NB7M requires conversion to 7Me-IEITC *in vitro* or can be directly incorporated into cancer cells.

The introduction of a tertiary butyl carbamoyl substituent onto the indole nucleus of NB7M may have endowed this molecule with resistance to intramolecular and/or intermolecular reactions leading to a significant increase (3x) in cytotoxicity versus 7-MeIEITC (Singh et al 2007). The unique stereo-electronic properties of the tertiary butoxy carbamoyl group may allow NB7M to interact more effectively with target proteins. This simple structural modification may also affect the kinetics of drug absorption in different cell lines, as suggested by the relative increased sensitivity to NB7M versus 7Me-IEITC in SMS-KCNR cells.

NB7M and its precursor 7Me-IEITC displayed strikingly similar effects on modulating the phosphorylation or expression of a multitude of molecular targets, including PI-3K and Akt, MAPKs ERK, p38, and JNK, and STAT-3 (Figure 4). Among these targets, the ability of NB7M to cause PI-3K/Akt/ERKs dephosphorylation (down-regulation) in conjunction with increased phosphorylation (up-regulation) of JNK, and p38, is mechanistically significant in the overall goal to development of NB7M as an antitumor agent against CNS cancers and neuroblastoma. Many types of tumors are associated with activated oncogenic kinases. These molecules play two complementary roles: (i) stimulation of signaling pathways that enable cells to function independently of their environment and, (ii) allow tumor cells to become resistant to genotoxic therapies (Hanahan and Weinberg 2000). For example, the serine/threonine kinase, Akt, and its family members are amplified or their activity is constitutively elevated in human carcinomas such as breast, pancreatic, ovarian, brain, prostate, and gastric adenocarcinomas (Nicholson and Anderson 2002). As it is a direct downstream target of phosphatidylinositol 3-kinase (PI3-K), Akt is also a key oncogenic survival factor and can phosphorylate and inactivate a panel of critical pro-apoptotic molecules, including Bad, caspase-9, the Forkhead transcription factor FKHRL1 (known to induce expression of pro-apoptotic factors such as Fas ligand), GSK3-β, cell cycle inhibitors p21 and p27, and tumor suppressor TSC2 (Nicholson and Anderson 2002). Akt can also inactivate p53, a key tumor suppressor, through phosphorylation and nuclear localization of MDM2 (Zhou et al 2001). Akt has also been shown to regulate the expression of p38 (Liao and Hung 2003). Thus, molecules

that can block Akt activity may play a significance role in cancer therapy and drug sensitization.

Akt plays an important role in cell survival and proliferation and has been strongly implicated in the development of resistance against chemotherapy agents such as paclitaxel, cisplatin, vincristine, and rapamycin in various human solid tumors (Kim et al 2005). It has also been shown that Akt is a direct target gene of STAT-3, which binds directly to its promoter to enhance its expression (Barre et al 2006). Because Akt is a well known positive mediator of cell survival, its up-regulation is likely to contribute to the antiapoptotic function of STAT-3 (Barre et al 2006).

Constitutive activation of STAT-3 has been reported in several primary cancers and tumor cell lines where it induces cell transformation through a combined inhibition of apoptosis and cell-cycle activation. Several studies have suggested that STAT-3 prevents cell-cycle arrest and cell death through up-regulation of survival proteins and down-regulation of tumor suppressors. STAT-3 inhibitors are being considered as cytotoxic drugs. Various STAT-3 inhibitors, such as cucurbitacin (Blaskovich et al 2003) and indirubin derivative (E804) (Nam et al 2005), induce apoptosis and display antitumor properties. Similarly, NB7M caused the down-regulation of STAT-3 in our *in vitro* treatments of NB (SMSKCNR and SH-SY5Y) cells. Unlike cucurbitacin and E804, which selectively inhibit STAT-3 expression, NB7M down-regulated the phosphorylation of PI-3K and Akt along with STAT-3. This broad effect could explain the pronounced cytotoxicity of NB7M in NB cell lines, specifically in resistant phenotype SMS-KCNR cells, as STAT-3 and Akt pathways have been implicated in the resistance of NB cells to cytotoxic drugs.

In contrast, JNK and p38 MAPKs are involved in the apoptotic response to cytotoxic agents (Mansouri et al 2003). Activation of p38 and JNK has been observed in human breast cancer cells treated with AplidinTM (Cuadrado et al 2003), a depsi-peptide molecule currently undergoing Phase 2 clinical trials. JNK mediates apoptosis induced by DNA-damaging drugs such as etoposide (VP-16) and Camptothecin in human myeloid leukemia cells (Brozovic and Osmak 2007) and vinblastine in KB3 lung carcinoma cells (Brozovic et al 2004). In MDA-MB-231 breast cancer cells, Taxol induced apoptosis via JNK, which causes inactivation of the antiapoptotic Bcl-2 protein (Wang et al 1999). Taxol has also been shown to increase p38 MAPK, ERK, and JNK activities in human breast cancer cells (Chen et al 1996). Similarly, our results suggest that NB7M suppresses pro-survival signaling and induces pro-apoptotic signaling in SMS-KCNR and SH-SY5Y NB cells (Figure 4).

The cytotoxic action of NB7M may be further explained by the fact that neuroblastoma cells (eg, SMS-KCNR and SH-SY5Y) accumulate and retain the more lipophilic NB7M and that this analog blocks the further progression of cells beyond the G1 phase. We observed that while the G1 population of NB7M treated SMS-KCNR cells slightly decreased, the S-phase population increased with increasing drug concentration. Hence, NB7M treatment prohibits the progression of treated SMS-KCNR cells to the G2/M checkpoint. Similarly, the progression of SH-SY5Y cells was halted at G1. Both NB cell lines (SMS-KCNR and SH-SY5Y) treated with sub-cytotoxic concentrations of NB7M, were prevented from entering the G2/M phase. This checkpoint is a known contributor to drug resistance since the G2/M checkpoint allows cells to repair potentially lethal damage such as single-strand DNA breaks. Thus, blocking the progression of unregulated dividing cells to the G2/M checkpoint reduces the possibility of repair and leads to increased cell death and potentially less drug resistance.

In summary, NB7M is cytotoxic to both CNS cancer cells and neuroblastoma. It also activates pro-apoptotic signaling, downregulates pro-survival signaling, promotes significant caspase activation, and regulates cell cycle progression. NB7M promotes apoptosis through multiple pathways, all of which are clinically relevant to the tumorigenesis and progression of ovarian and other cancers. This broad range of biological activities underscores the in vitro efficacy of NB7M in both CNS cancers and neuroblastoma and warrants further development of this drug as an anticancer agent.

Acknowledgments

This work was supported by funds from a NICHD, K12 HD043447 BIRCWH Scholar Grant to Dr. Brard. The authors thank Dr. Sunil K Shaw for advice and technical guidance and NIH COBRE Grant 1-P20RR018728 for providing instrumentation support.

References

Barre B, Vigneron A, Perkins N, et al. 2006. The STAT-3 oncogene as a predictive marker of drug resistance. *Trends in Mol Med,* 13:4–11.

Blaskovich MA, Sun J, Cantor A, et al. 2003. Discovery of JSI-124 (Cucurbitacin I), a selective janus kinase/signal transducer and activator of transcription 3 signaling pathway inhibitor with potent antitumor activity against human and murine cancer cells in mice. *Cancer Res,* 63:1270–9.

Brodeur GM, Pizzo PA, Poplack DG. 2001. Principles and Practice of Pediatric Oncology (Neuroblastoma). Philadelphia: 4th Edition. Lippencott-Raven, pp. 895–937.

Brozovic A, Osmak M. 2007. Activation of mitogen-activated protein kinases by cisplatin and their role in cisplatin-resistance. *Cancer Lett*, 251:1–6.

Brozovic A, Fritz G, Christmann M, et al. 2004. Long-term activation of SAPK / JNK, p38 kinase and fas L-expression by cisplatin is attenuated in human carcinoma cells that acquired drug resistance. *Int J Cancer*, 112:974–85.

Chen YR, Wang X, Templeton D, et al. 1996. The role of c-Jun N-terminal kinase (JNK) in apoptosis induced by ultraviolet C and Y-radiation. *J Biol Chem*, 271:3192–9.

Conaway CC, Yang MY, Fung LC. 2002. Isothiocyanates as cancer chemopreventive agents: their biological activities and metabolism in rodents and humans. *Curr Drug Metabol*, 3:233–55.

Cuadrado A, Garcıa FLF, Gonzalez L, et al. 2003. Aplidin™ induces apoptosis in human cancer cells via glutathione depletion and sustained activation of the epidermal growth factor receptor, Src, JNK, and p38 MAPK. *J Biol Chem,* 278:241–50.

Dick RA, Kensler TW. 2002. Chemoprotective potential of phase 2 enzyme inducers. *Exp Rev of Anticancer Ther,* 2:581–92.

Garcia H, Brar GA, David HH, et al. 2005. Indole-3-carbinol (I3C) Inhibits cyclin-dependent kinase-2 function in human breast cancer cells by regulating the size distribution, associated cyclin-E forms, and subcellular localization of the CDK2 protein complex. *J Biol Chem*, 280:8756–64.

Goldsby RE, Matthay KK. 2004. Neuroblastoma, evolving therapies for a disease with many faces. *Paed Drugs*, 6:107–22.

Hanahan D, Weinberg RA. 2000. The hallmarks of cancer. *Cell,* 100:57–70.

Jackson SJ, Singletary KW. 2004. Sulforaphane inhibits human MCF-7 mammary cancer cell mitotic progression and tubulin polymerization. *J Nutr*, 134:2229–36.

Jackson SJ, Singletary KW, Venema RC. 2007. Sulforaphane suppresses angiogenesis and disrupts endothelial mitotic progression and microtubule polymerization. *Vascul Pharmacol,* 46:77–84.

Jakubikova J, Bao Y, Sedlak J. 2005. Isothiocyanates induce cell cycle arrest, apoptosis and mitochondrial potential depolarization in HL-60 and multidrug-resistant cell lines. *Anticancer Res*, 25:3375–86.

Jakubikova J, Sedlak J, Bod'o J, et al. 2006. Effect of isothiocyanates on nuclear accumulation of NF-kappaB, Nrf2, and thioredoxin in caco-2 cells. *J Agric Food Chem*, 54:1656–62.

Johnson CR, Chun J, Bittman R, et al. 2004. Intrinsic cytotoxicity and chemomodulatory actions of novel phenethylisothiocyanate sphingoid base derivatives in HL-60 human promyelocytic leukemia cells. *J Pharma Exp Ther,* 309:452–61.

Kalkunte S, Swamy N, Brard L, et al. 2006. Benzyl isothiocyanate (BITC) induces apoptosis in ovarian cancer cells in vitro. *J Exp Ther Oncol*, 5:287–300.

Kasibhatla S, Amarante-Mendes GP, Finucane D. 2006. Green staining of suspension cells with Hoechst 33258 to detect apoptosis. *CSH Protocols*, doi:10.1101/pdb.prot4492.

Kim D, Cheng GZ, Lindsley CW, et al. 2005. Targeting the phosphatidylinositol-3 kinase/Akt pathway for the treatment of cancer. *Curr Opin Invest Drugs*, 6:1250–8.

Liao Y, Hung MC. 2003. Regulation of the activity of p38 mitogen-activated protein kinase by Akt in cancer and adenoviral protein E1A-mediated sensitization to apoptosis. *Mol Cell Biol*, 23:6836–48.

Malich G, Markovic B, Winder C. 1997. The sensitivity and specificity of the MTS tetrazolium assay for detecting the in vitro cytotoxicity of 20 chemicals using human cell lines. *Toxicol,* 124:179–92.

Mansouri A, Ridgway LD, Korapati AL, et al. 2003. Sustained activation of JNK/p38 MAPK pathways in response to Cisplatin leads to Fas ligand lnduction and cell death in ovarian carcinoma cells. *J Biol Chem*, 278:19245–56.

Matthay KK, Villablanca JG, Seeger RC, et al. 1999. Treatment of high-risk neuroblastoma with intensive chemotherapy, radiotherapy, autologous bone marrow transplantation, and 13-*cis*-retinoic acid, *N Engl J Med,* 341:1165–73.

Mazumder S, DuPree EL, Almasan A. 2004. A dual role of cyclin E in cell proliferation and apoptosis may provide a target for cancer therapy. *Curr Cancer Drug Targets*, 4:65–75.

Nam S, Buettner R, Turkson J, et al. 2005. Indirubin derivatives inhibit STAT-3 signaling and induce apoptosis in human cancer cells. *PNAS*, 102:5998–6003.

Nicholson KM, Anderson NG. 2002. The protein kinase B/Akt signaling pathway in human malignancy. *Cell Signal*, 14:381–95.

Perez CA, Matthay KK, Atkinson JB, et al. 2000. Biologic variables in the outcome of stages I and II neuroblastoma treated with surgery as primary therapy: A children's cancer group study. *J Clin Oncol*, 18:18–26.

Pines J. 1999. Four-dimensional control of the cell cycle. *Nature Cell Biol*, 1:73–9.

Salvesen GS, Abrams JM. 2004. Caspase activation – stepping on the gas or releasing the brakes? Lessons from humans and flies. *Oncogene*, 23:2774–84.

Satyan KS, Swamy N, Dizon DS, et al. 2006. Phenethyl isothiocyanate (PEITC) inhibits growth of ovarian cancer cells by inducing apoptosis: Role of caspase and MAPK activation. *Gynecol Oncol***,** 103:261–70.

Serova M, Galmarini CM, Ghoul A, et al. 2007. Antiproliferative effects of sapacitabine (CYC682) a novel 2'-deoxycytidine-derivative, in human cancer cells, *Br J Cancer,* 97:628–36.

Singh RK, Lange TS, Kim KK, et al. 2007. Effect of indole ethyl isothiocyanates on proliferation, apoptosis, and MAPK signaling in neuroblastoma cell lines, *Bioorg Med Chem Lett*, 17:5846–52.

Singh RK, Lange TS, Kim KK, et al. 2008. A novel indole ethyl isothiocyanate (7Me-IEITC) with anti-proliferative and pro-apoptotic effects on platinum-resistant human ovarian cancer cells. *Gynecol Oncol*, Mar 7: In press.

Tseng E, Kamath A, Morris ME. 2004. Effect of organic isothiocyanates on the P-Glycoprotein- and MRP1-mediated transport of daunomycin and vinblastine. *Pharm Res*, 19:1509–15.

Van EM, Ramaekers FC, Schutte B, et al. 1996. A novel assay to measure loss of plasma membrane asymmetry during apoptosis of adherent cells in culture. *Cytometry*, 24:131–9.

Wang TH, Popp DM, Wang HS, et al. 1999. Microtubule dysfunction induced by paclitaxel initiates apoptosis through both c-Jun N-terminal kinase (JNK)-dependent and -independent pathways in ovarian cancer cells. *J Biol Chem*, 274:8208–16.

Yuesheng Z, Tang L, Gonzalez V. 2003. Selected isothiocyanates rapidly induce growthinhibition of cancer cells. *Mol Canc Therap*, 2:1045–52.

Zhou BP, Liao Y, Xia W, et al. 2001. HER-2/neu induces p53 ubiquitination via Akt-mediated MDM2 phosphorylation, *Nature Cell Biology,* 3:973–82.